Performance Evaluation of Bolt-Cutter System on First Taurus Launch

15 October 1994

Prepared by

F. BABAN, R. WILLIAMS, S. AMIMOTO,
W. HANSEN, and T. BIXLER
Mechanics and Materials Technology Center
Technology Operations

DTIC
ELECTE
S
FEB 2 8 1995
G
D

Prepared for

SPACE AND MISSILE SYSTEMS CENTER
AIR FORCE MATERIEL COMMAND
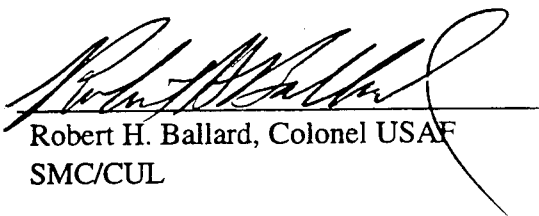2430 E. El Segundo Boulevard
Los Angeles Air Force Base, CA 90245

Programs Group

19950222 005

**THE AEROSPACE
CORPORATION**
El Segundo, California

Robert H. Ballard, Colonel USAF
SMC/CUL

REPORT DOCUMENTATION PAGE

Public reporting burden for this collection of information is estimated to average 1 hour per response, including the time for reviewing instructions, searching existing data sources, gathering and maintaining the data needed, and completing and reviewing the collection of information. Send comments regarding this burden estimate or any other aspect of this collection of information, including suggestions for reducing this burden to Washington Headquarters Services, Directorate for Information Operations and Reports, 1215 Jefferson Davis Highway, Suite 1204, Arlington, VA 22202-4302, and to the Office of Management and Budget, Paperwork Reduction Project (0704-0188), Washington, DC 20503.

1. AGENCY USE ONLY (Leave blank)	2. REPORT DATE 15 October 1994	3. REPORT TYPE AND DATES COVERED

4. TITLE AND SUBTITLE

Performance Evaluation of Bolt-Cutter System on First Taurus Launch

5. FUNDING NUMBERS

F04701-93-C-0094

6. AUTHOR(S)

F. Baban, R. Williams, S. Amimoto, W. Hansen, and T. Bixler

7. PERFORMING ORGANIZATION NAME(S) AND ADDRESS(ES)

The Aerospace Corporation
Technology Operations
El Segundo, CA 90245-4691

8. PERFORMING ORGANIZATION REPORT NUMBER

TR-94(4508)-1

9. SPONSORING/MONITORING AGENCY NAME(S) AND ADDRESS(ES)

Space and Missile Systems Center
Air Force Materiel Command
2430 E. El Segundo Boulevard
Los Angeles Air Force Base, CA 90245

10. SPONSORING/MONITORING AGENCY REPORT NUMBER

SMC-TR-95-3

11. SUPPLEMENTARY NOTES

12a. DISTRIBUTION/AVAILABILITY STATEMENT

Approved for public release; distribution unlimited

12b. DISTRIBUTION CODE

13. ABSTRACT (Maximum 200 words)

In rapid response to the request of the Space Test and Experimentation Directorate in Space Launch Operations, a launch-critical experimental investigation was conducted to evaluate the performance of a particular bolt-cutter system for separating stages on the first Taurus launch. The tests were to examine the variation of tension preloading on the bolt system and to demonstrate the tolerable margin on this parameter for such launches with the new types of bolts since the preloading was known to vary as much as 12% from a preset value before launch. We planned and carried out the experiment, designed and assembled the fixture to properly simulate flight application, and developed diagnostics. Four bolt cutters were purchased from the manufacturer for these tests, and one was provided by the contractor. In addition to the obvious requirement to demonstrate the successful severing of bolts under varying preloads, ignition-wire current and timing of chisel impact on the bolt were monitored. An optical diagnostic was designed to determine the flyout velocity and kinetic energy of the broken pieces. These latter measurements will be useful in anchoring performance codes simulating and assessing the structural dynamics of the bolt-cutter function for future missions.

The tests were conducted successfully and the bolts were severed successfully in all five tests. The preloads were successively lowered from 2,500 lb to 2,250, 2,000, 1,500, and 1,000 lb These tests contributed in a timely manner to the STEP launch decision and to launch mission assurance. They demonstrated important margin to the nominally set 3,200 lb. preload. The entire complicated experimental program from inception to completion was accomplished in less than three weeks.

14. SUBJECT TERMS

Bolt-cutter, Taurus, Stage-separation

15. NUMBER OF PAGES

35

16. PRICE CODE

17. SECURITY CLASSIFICATION OF REPORT UNCLASSIFIED	18. SECURITY CLASSIFICATION OF THIS PAGE UNCLASSIFIED	19. SECURITY CLASSIFICATION OF ABSTRACT UNCLASSIFIED	20. LIMITATION OF ABSTRACT

DTIC QUALITY INSPECTED 4

Preface

Accesion For		
NTIS CRA&I	☒	
DTIC TAB	☐	
Unannounced	☐	
Justification ⎯⎯⎯⎯⎯		
By ⎯⎯⎯⎯⎯⎯⎯		
Distribution /		
Availability Codes		
Dist	Avail and / or Special	
A-1		

Contents

Figures

Tables

1. Introduction

At the request of the Space Test and Experimentation Directorate of Space Launch Operations, an experimental investigation was undertaken to evaluate the capability of a particular bolt cutter in severing the accompanied bolt. The bolt cutter was used for separating the stages on the first Taurus launch (Figure 1). The Taurus payload consisted of two satellites—Space Test Experiment Platform (STEP) Mission-0 and DARPASAT. The bolts used for separating these two satellites were identical from a metallurgical point of view. However, the preload tensions to which the bolts were subjected were different. The preload set on the bolts separating STEP Mission-0 satellite were set at 3200 lb, while the tension on DARPASAT bolts nominally exceeded 4200 lb. Each cutter consists of a chisel that is propelled into the bolt by an explosive powder mixture. Ammonium perchlorate is the main igniting chemical ingredient of the explosive powder. A bridge-wire buried inside the powder is exploded by running a 5-A current for a minimum duration of 10 ms. Detonation occurs immediately after the bridge-wire burns out. The explosion drives the chisel onto the bolt, which is held securely in an anvil (Figure 2).
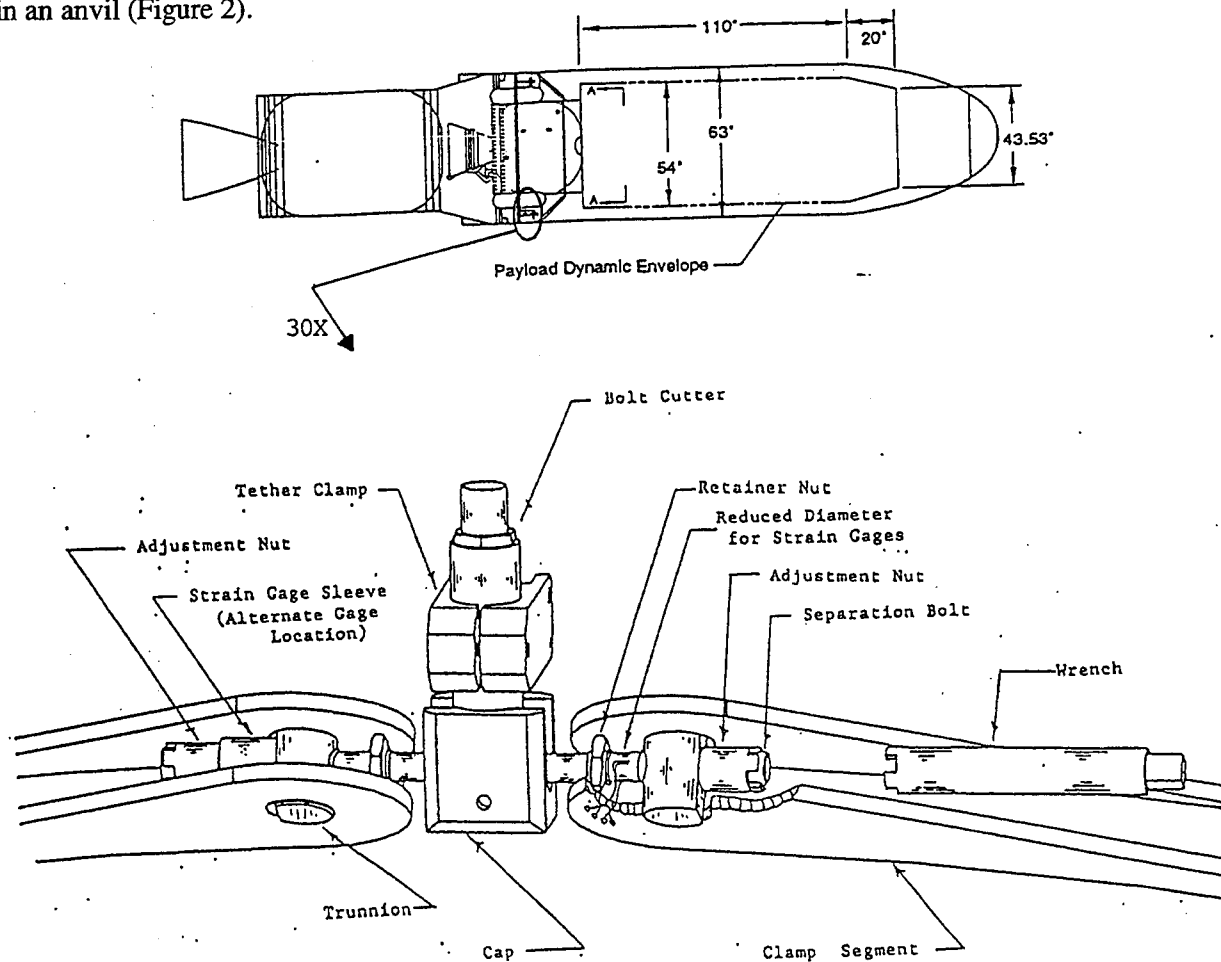
Figure 1.   Taurus payload, Space Test and Experimentation Platform (STEP), and the exploded view of the bolt cutter used for separating the payload from the vehicle.

1
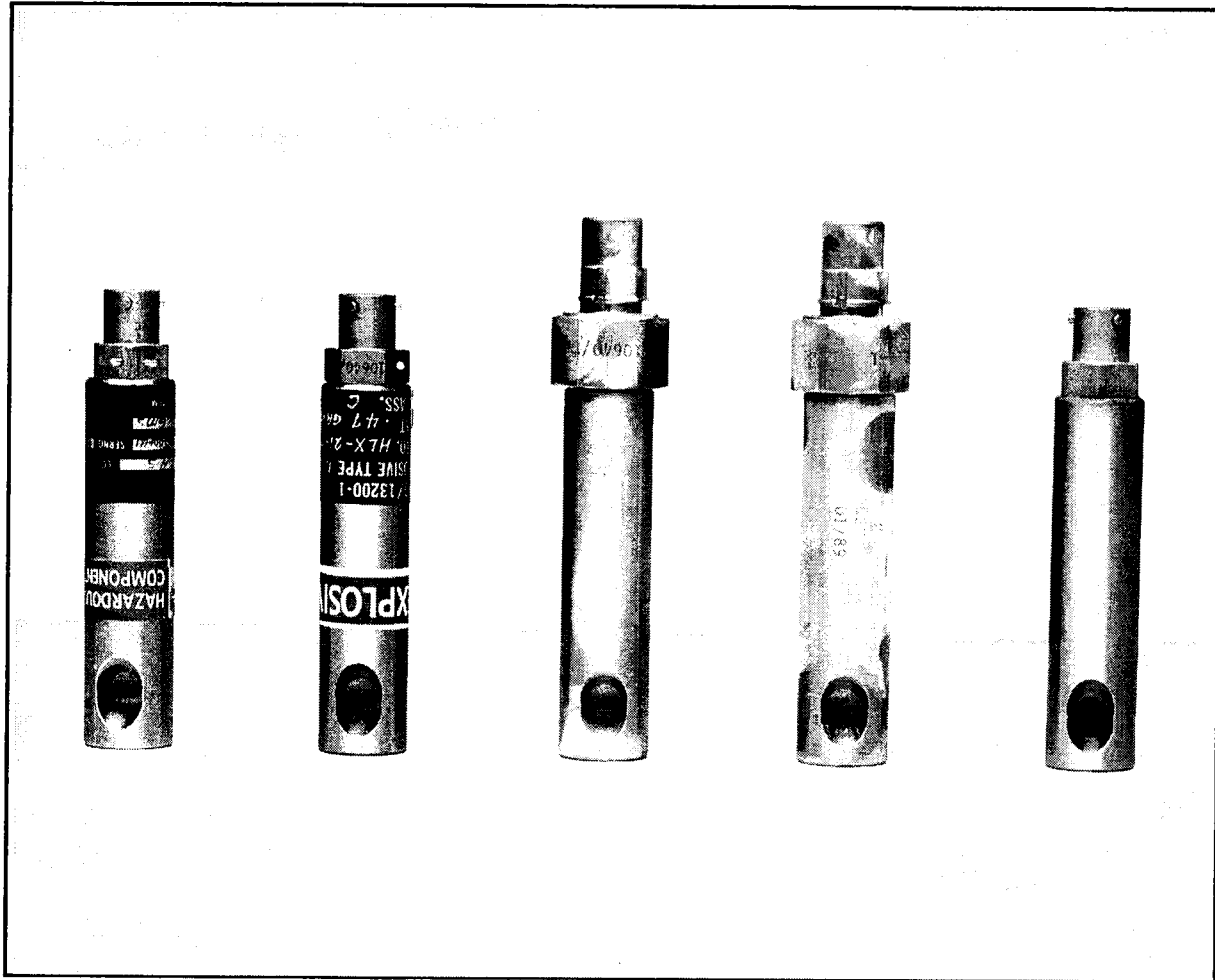
Figure 2. Photograph of bolt cutters used.

A number of bolt cutters of this class had been repeatedly used in previous launches. The bolts used in previous launches had all been specified to be A286-stainless steel, cold worked and heat treated to 180–210 ksi. However, the bolts used for staging in this launch were not cold-worked hardened and were specified to be heat treated only to 160 ksi. In an attempt to demonstrate that the cutter is capable of severing these new bolts, the contractor was forced to run a series of tests. Although the cutters managed to sever the bolts in many cases, there were times that the cutter failed to sever the bolt. The contractor's explanation for these failed cases was that the bolts were not subjected to the proper preload (tension) at the time the chisel impacted them. In other words, the bolts are required to be preloaded to a certain threshold value for the cutter to sever them successfully. This brought up an additional concern and posed the following question: "What is the minimum required preload on the bolt for successful severing?" Furthermore, it has been observed that the preload set on the bolts had been changed by as much as 12% due to shipment. This brings about another concern: "How much will the set preload change during launch? i.e., What is the margin in the set tension?"

2

bolt for successful severing?" Furthermore, it has been observed that the preload set on the bolts had been changed by as much as 12% due to shipment. This brings about another concern: "How much will the set preload change during launch? i.e., What is the margin in the set tension?"

To answer these questions and to assess the margin of reliability in using these bolt cutters with the accompanied bolts, a series of tests was conducted in our lab. Room 1200D was designated to be the test cell since the walls in this room are made of 12-in.-thick concrete. An explosion-proof safe was made available to store the cutters, which are classified as class-C explosives. Four bolt cutters were purchased from the sole manufacturer (Quantic Industries). An additional bolt cutter was provided by the contractor, DSI (Figure 2). The operational procedures were written, and permission for conducting the experiment was obtained. A fixture was promptly designed, fabricated, and assembled to accommodate the bolt cutter and hold the bolt securely with the desired tension. Several diagnostics were employed to obtain much-needed additional information, such as the time of impact of the chisel on the bolt relative to the bridge-wire burn out, and the velocity and the kinetic energy of the broken bolts flying out of the fixture.

2. Experimental Setup

The test apparatus consisted of the following: a customized fixture for loading the bolt and appropriately positioning the cutter, an optical "time-of-flight" diagnostic used to measure the flyout velocity of a severed bolt segment, a remotely triggered current pulser (5 A, 10 ms) used to detonate the bridge wire of the cutter's explosive, and a video monitoring setup that provided remote visual access as well as a record of test firings. These items were assembled on a 3 ft × 5 ft optical table. A plastic tent was used to shroud the table during firings in order to confine and exhaust potentially toxic gases through an external hood. Figure 3 is a photograph of the experimental setup.
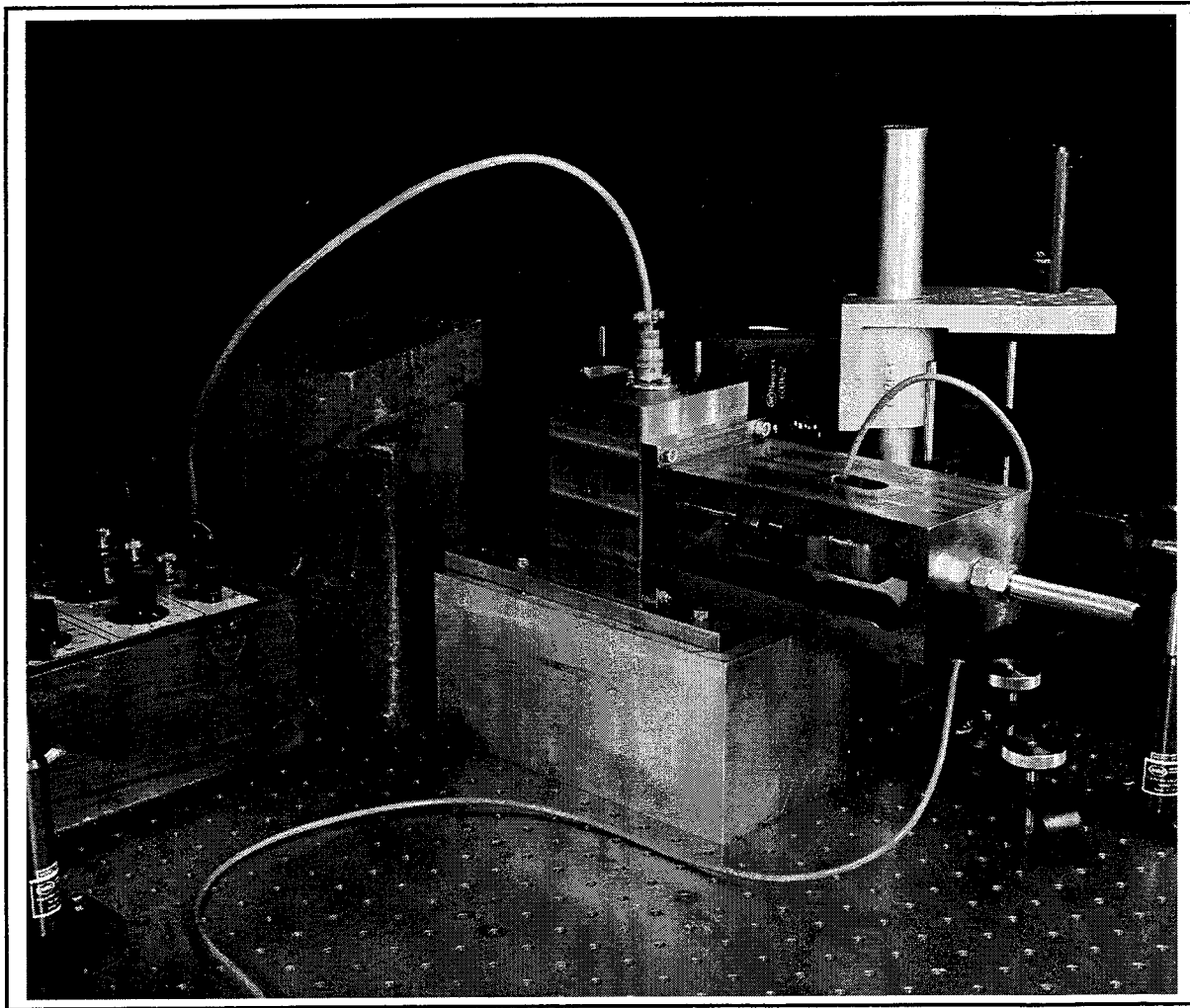
Figure 3. Experimental setup.

The test fixture (Figure 4) designed to study the severance of an A286-stainless-steel bolt was required to simulate the physical parameters encounter by the bolt-cutter arrangement on the Taurus V-band. Significant parameters included minimal restriction of cutter motion perpendicular to the bolt, firm vertical support of the bolt at locations on both sides of the cutter, and minimal restrictions to horizontal bolt motion following severance. In addition, the axial load applied to the bolt needed to be accurately applied and measured.

The main body of the test fixture was fabricated from 303 stainless steel (SS) and provided a vertically oriented cavity for insertion of the cutter and a horizontal cavity for insertion of the bolt through the cutter. Bushings fabricated from precipitation-hardened 17-4 SS provided vertical support for the bolt at both ends of the horizontal cavity. These bushings were free to move horizontally with the severed bolt pieces following cutter operation. Contact between the bolt and anvil portion of the cutter was ensured by compressing a spring beneath the cutter during bolt/cutter installation. The spring provided a minimal restriction to the vertical motion of the cutter.

The load cell strut was horizontally attached to one side of the test fixture's main body. This provided an enclosure for the load cell and bolt collar. Axial loads were applied by screwing the loading bolt into the load cell. The load cell was restricted from rotation during loading to avoid applying torsion to the A286 bolt. Output from the load cell was monitored to verify proper loading. Axial motion of the loading bolt, load cell, and bolt collar was prevented by securing the restrictor nut against the inner wall of the load cell strut, following A286 bolt loading.

Free axial motion of the A286 bolt following severance was provided for both severed segments. The segment facing the load cell was free to move within the bolt collar. The bolt collar incorporated an internal relief, permitting free flight of the severed bolt. This provided a means of loading the A286
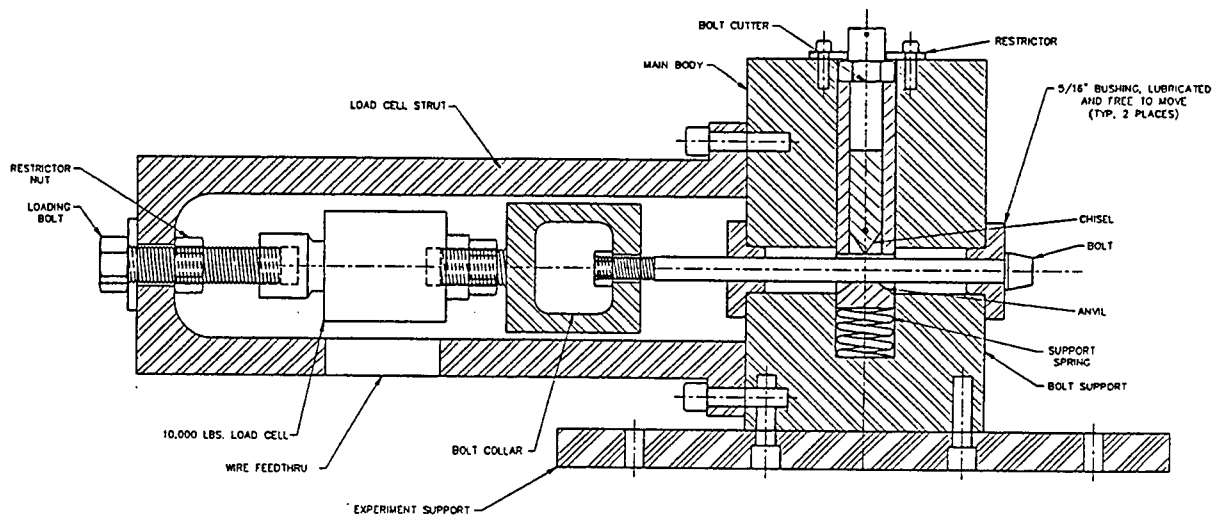
Figure 4. Schematic of test fixture for severing bolts and applying desired preload.

6

bolt and load cell without adding the mass of the load cell to the A286 bolt. This was a critical feature since the inclusion of additional mass would have increased the mass of the severed bolt segments. The other A286 bolt segment was free to fly away from the test fixture in order to provide access for exit velocity measurements. This segment was stopped by an arrangement of lead bricks placed approximately one foot away from the test fixture.

3. Diagnostics

In order to adequately test the function of the bolt cutter, a variety of analytical techniques was employed. First-order requirements necessitated an accurate measurement of A286 bolt preload. Secondary requirements included timing of cutter events (i.e., time lag between explosive charge detonation and complete bolt severance) as well as the determination of kinetic energy imparted to bolt segments following severance. The latter applied a laser-based time-of-flight diagnostic used to interpret bolt separation velocity.

Accurate preloading of the A286 bolts was critical to determining flight worthiness of the bolt cutter. The cutter's margin of reliability was predicated on verification of A286 bolt severance at bolt preloads less than nominal flight preload. A load cell (Transducers, Inc. Model T182-10K-10P1) rated for 10,000 lb was employed to measure bolt preload. The load cell was calibrated over a range of 0 to 3000 lb with the assistance of a Reihle tensile tester and Reihle load cell. Accuracy of the control load cell was ± 1% full scale (10,000 lb). Linearity and minimal hysterisis was verified for the Transducers, Inc. load cell by cyclically loading the cell and comparing output with the control load cell.

Observation of cutter event timing was pursued with three diagnostic tools. The load cell was designed to measure high-frequency load oscillations, which provided an accurate measurement of deloading following bolt severance. This timing mark was compared with burnout of the explosive's bridge-wire to provide a correlation between cutter detonation and bolt severance. A second technique of providing the same correlation was applied by stretching a 30-gauge wire across the A286 bolt-head held within the bolt collar. This breakwire served as an electrical connector in a simple resistor/battery circuit. Acceleration of the bolt head following severance split the wire and extinguished the circuit's output. This technique was assumed to be more accurate than the load cell response because of the reduction in coupling mechanical components. But, as Table 1 indicates, the breakwire timing technique lags the load cell signal in an inconsistent manner. This may be attributed to varying breakwire tension prior to severance and differing bolt segment velocities.

As a third technique, the time-of-flight diagnostic (described below) was placed adjacent to the bolt head on the free end of the test fixture. Bolt movement decreased laser intensity and provided a timing comparison with cutter detonation. The measurements appear to correlate well with load cell data.

Table 1. Detonation / Severance Timing

Test No.	Load Cell (ms)	Break-wire (ms)	Time of Flight (ms)
1	N/A	N/A	N/A
2	1.50	N/A	1.36
3	1.30	1.60	1.40
4	1.50	1.65	1.39
5	0.90	N/A	N/A

The time-of-flight diagnostic consisted of a 0.5-mW He-Ne laser split into two beams of approximately equal intensities (Figure 5). The beams were located such that the first and then the second would be interrupted when the "b" end of the bolt flew out of the test fixture after the chisel blade was fired. By definition, the "b" end was the segment on which the time-of-flight measurements were performed. To prevent frictional air losses from affecting the measurements, the He-Ne beams were located close to the "b" end of the bolt, generally 0–4 mm for the first beam and an additional 15–17 mm for the second beam. This also ensured that the bolt's trajectory would not change significantly as it passed through the time-of-flight beam positions. The beams were then recombined onto a single silicon photodiode/amplifier (New Focus model 1601), and its output was recorded on a 100-MHz bandwidth oscilloscope using a pre-trigger record mode.

The test setup was tested by passing a small stick or a ball driver tool rapidly across the two beams. Oscillograms recorded in this way showed a sharp step decrease to the 50% light intensity level when the first beam was broken. When the second beam was broken as the first remained broken, the signal took another step decrease to zero (obviously, the bolt or the stick was longer than the separation
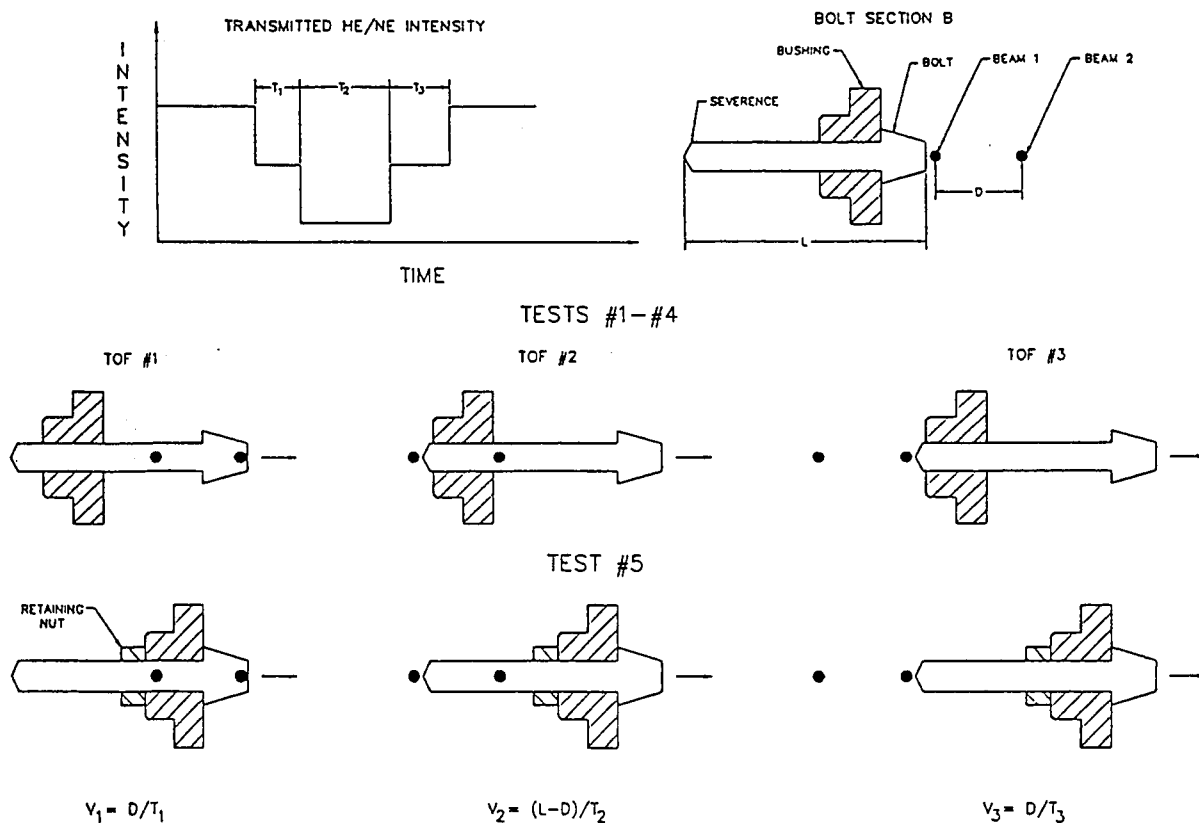
Figure 5.   Velocity calculation based on the signal obtained from photodiode, separation distance of two laser beams (D), and the length of the broken bolt (L).

10

distance of the two beams). As the bolt ceased to interrupt both beams and allowed only one beam to pass, the signal stepped back up to the 50% and then with both beams unbroken to the 100% level (Figure 6). The effects of additional light and vibration during an actual experimental run could lead to slight inaccuracies in the interpretation of the data. In each case, the "b" end of the bolt, the bushing, and the nut were recovered for mass and length measurements. The clearance of the bushing and the rod was 1 mil. The bushings were found to be firmly stuck onto the bolt near the severed end of the "b" end due to the plastic deformation in the bolt caused by the impact of the chisel.

A Sony black and white video camera (model XC-57) and a JVC video recorder were used to record each test. The camera was located about 4 ft from the test fixture. A short-focal-length lens was used to provide a large field of view. The recorded images were digitized and time-base corrected before printing.
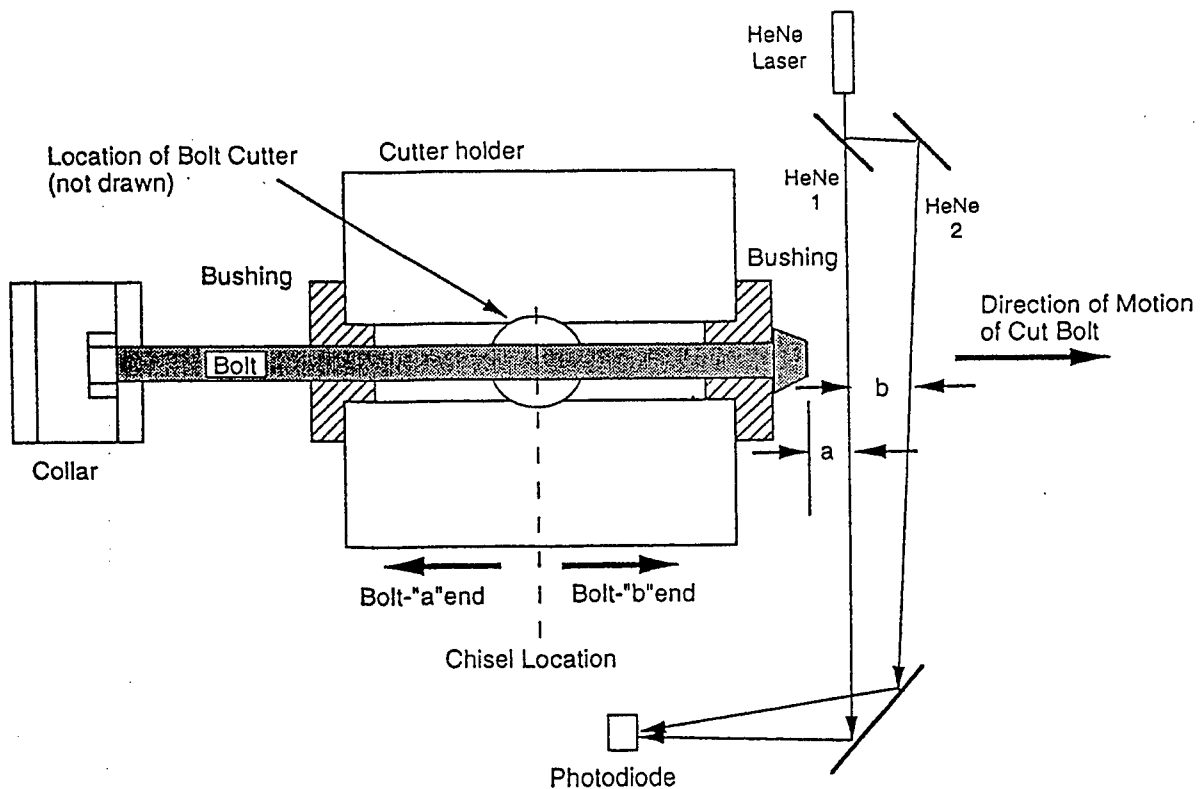
Figure 6.   Time-of-flight layout. This cut-away view shows the location of the chisel and the locations of He-Ne beams 1 and 2. The "b" end of the bolt and the sliding bushing will intercept the He-Ne beams as it emerges from the cutter hole (fixture). The timing information is detected on the photodiode and recorded on an oscilloscope. Dimensions a, the separation of the edge of the "b" end of the bolt and He-Ne beam 1, and b, the separation of the He-Ne beams, in path of the emerging bolt, are given in Table 3 for each bolt-cutter test.

11

4. Data Analysis

The analysis of the time-of-flight data begins with the classical analysis of conversion of potential energy to kinetic energy when two masses are separated, or a solid body is fragmented into two pieces. In our tests, the potential energy came from stored elastic deformation of the bolt during and immediately after severance. This potential energy was converted to kinetic energy when the "a" and "b" ends of the severed bolt flew out. Invoking conservation of momentum and conservation of energy,

$$m_a v_a = m_b v_b \tag{1}$$

$$KE_a + KE_b = m_a v_a^2 / 2 + m_b v_b^2 / 2 = \text{constant} \tag{2}$$

From time-of-flight measurements, the velocity of the "b" end, v_b, can be measured, and the masses m_a and m_b measured after the bolt is cut. The bushing for Tests 1–4 was allowed to slide on the bolt, but for Test 5, the bushing was locked in place using nuts on both sides of the bushing. For the first four tests, the recovered "b" end of the bolt always had its bushing firmly attached to the bolt near the cut. Several assumptions could be tested for each portion of the oscilloscope trace. The velocity can be inferred from the three segments of the observed oscillogram. In segment 1, the velocity of the bolt can be calculated by dividing the separation distance between the He-Ne beams by the timed length of the first 50% intensity step (Figure 6). No information is directly observable for the bushing velocity. In the second segment, where both beams are blocked, the velocity is calculated by taking the difference between the "b" bolt length and the separation of the He-Ne beams and dividing by the time for the zero intensity time length. Again, no information is directly observed for the bushing velocity. The third segment, corresponding to the 50% intensity level, is defined by the back end of the bolt that clears both beams. Hence, the velocity is calculated by dividing the He-Ne separation by the time duration of the third segment. Again, no direct knowledge of the bushing velocity is evident.

The bushing velocity may be inferred by the following procedure. We can assume that either the bolt alone is moving, or that the bolt and bushing are moving together. In calculating the kinetic energy, the mass of the moving "b" bolt end, or the mass of the "b" end with bushing are used in each segment. As will be shown, the assumption that in segment 1, only the bolt is moving, and in segment 2, both bushing and bolt are moving seems to be most consistent with the energy conservation requirement. Finally the total kinetic energy of the cut pieces can be calculated using the above equations.

$$KE_a + KE_b = KE_b (1 + m_b / m_a) \tag{3}$$

By assuming that the velocity of the chisel is approximately 6000 in./s, and its mass is 0.01653 kg, the chisel kinetic energy is 190 J. The fraction of transferred kinetic energy can be estimated by dividing the sum of kinetic energy in both bolt halves by the chisel kinetic energy. The chisel also has enough kinetic energy to impact the anvil, leaving a permanent deformation once the bolt halves fracture and move apart. If the chisel position is known as a function of time, the kinetic energy before and after

fracture as well as during penetration of the bolt can be determined. Thus, the energy budget of the bolt-cutting process can be established. However, the agreed-upon test conditions excluded modifications to the bolt cutter necessary to measure the chisel position as a function of time for this test series.

One additional source of potential energy was considered, namely, the elastic energy in the tension from pre-loading of the bolt. Estimates were made for this value for a nominal 2500-lb load using the stiff 3-in. × 3-in. block test fixture. The estimated stored energy was much less than 0.1 J, which can be safely ignored for the time-of-flight measurements.

5. Summary of Tests

Five tests were conducted to examine the variation of tension preloading on the bolt-cutter system and to demonstrate a tolerable margin for this parameter. The preloads were successively lowered from 2,500 lb to 2,250, 2,000, 1,500, and 1,000 lb. Prior to tabulating and discussing the results, a summary for each run will be given to familiarize the reader with the general condition of the test and the diagnostics employed.

5.1   Run 1

The first test was a success in that the bolt cutter severed the bolt under 2500 lb preload. The tested unit was the cutter furnished by DSI (P/N 13200). The bolt was a salvaged portion of an actual V-band bolt that had been previously cut by DSI. The bolt was modified (i.e., re-threaded), and its dimensions and weight were carefully measured before the test. These measurements were repeated for both portions of the bolt after it was cut. Our diagnostics included a strain gage mounted on the nut securing the bolt to the fixture, the load-cell, and a two-beam laser system for time-of-flight measurement to obtain the speed of the cut portion of the bolt. The signals were recorded on digital scopes. The ignition signal from the constant-current circuit was also recorded on a digital scope.

The strain-gage signal was not received. Wires connecting the strain gage to instrumentation were sheared off during bolt severance. Regardless, we devised an alternate method to obtain the same information. The signals from the load-cell and the constant-current pulser were received. The signals observed were as expected. Unfortunately, the signals were erased before the hard prints could be obtained. The time-of-flight measurements were successfully recorded. Based on the distance between the two laser beams and the time it took for the broken bolt to fly across the two beams, the velocity of the flying portion of the bolt was calculated.

5.2   Run 2

The cutter once again severed the bolt successfully. The preload on the bolt for Test 2 was set at 2250 lb. The bolt cutter was a 13200 type purchased from Quantic Industries Inc. The bolt was similar to the one tested in run No.1. It was a salvaged portion of a broken V-band bolt provided by DSI. The bolt had been re-threaded and made ready for the test.

The diagnostics were basically the same as those used in Test 1. However, instead of using the strain gage, which failed to provide any information in Test 1, a thin wire (32-gauge) was stretched immediately downstream of the bolt, and a small current was run through the wire. We anticipated that the thin wire would break upon the impact of the cutter on the bolt. The current running through the wire was monitored on one channel of the scope. A slight adjustment was also made to the time-of-flight measurement system. The two laser beams were translated closer to the bolt such that the first beam was immediately adjacent to the head of the bolt. This was done to infer the time at which the bolt was cut. Other preliminary measurements, such as weight and dimensions of the bolt, bushing, nut, and washer, were made prior to the test.

15

Post-mortem analysis included the measurements of weight and length of the broken bolt, velocity of the flying portion of the bolt, and the time between the bridge-wire burn out and the cutter impact on the bolt.

5.3   Runs 3 & 4

The bolt cutters successfully severed the bolts in both runs. The preload on the bolt for Test 3 was set at 2000 lb; while in Test 4, the bolt was subjected to 1500 lb tension. The bolt cutters had been purchased from Quantic Industries Inc. (P/N 16108). These cutters were slightly different from the ones used in Tests 1 and 2. The difference was only in the electrical connection where the current was supplied to the cutter. The pin connections were slightly different, and the connector itself was bulkier. This necessitated a slight modification of our fixture to accommodate the bulkier connector. The bolts in these tests were both salvaged portions of two broken DARPASAT bolts furnished by DSI. They had been re-threaded and made ready for these tests. From a metallurgical point of view, they were identical to the bolts used in Tests 1 and 2 (A286 stainless steel; not cold-work hardened).

The diagnostics were basically the same as those used in Test 2. Once again, a thin break-wire (32-gage) was stretched immediately downstream of the bolt, and a small current was run through the wire. The break wire was to provide the time at which the broken bolts began flying out of the fixture. The time-of-flight measurement system with the two laser beams was used in both tests to infer the time at which the bolts were cut, as well as to assess the velocity of the flying portion of the bolts. Other preliminary measurements, such as weight and dimensions of the bolts, bushings, nuts, and washers, were made prior to the test.

Post-mortem analysis included the measurements of weight and length of the broken bolts, velocity of the flying portion of the bolt, and the time between the bridge-wire burn out and the movement of the bolts.

5.4   Run 5

The fifth test was conducted. The bolt cutter successfully severed the bolt. The preload on the bolt for this test was set at 1000 lb. The cutter was purchased from Quantic Industries. The unit came in two pieces: the cartridge and the electronic connector head. The head was mounted onto the cartridge and torqued to the manufacturer's specification (65 in.-lb). The bolt was made of a stainless-steel rod (5/16 in. diam.). It had been cut to the proper length (6 in.) and threaded from both ends in our own shop. From a metallurgical point of view, this bolt was identical to the bolts used in previous tests (A286 stainless steel; not cold-work hardened).

Slight modifications were made in our measurement techniques. In light of the fact that the time of chisel impact is more informative than the time at which the bolt breaks, the thin break-wire was stretched immediately above the bolt on the path of the chisel. In other words, the wire was placed such that the chisel would break the wire just prior to impacting the bolt. In so doing, the velocity of the chisel could be determined by obtaining the lag time between the breakage of the wire and the bridge-wire burn out. The time-of-flight measurement system with the two laser beams was once again used in this test to assess the velocity of the flying portion of the bolts. However, due to the fact that in previous tests, there was some ambiguity with regard to the velocity of the bolt relative to

the velocity of the bushing, in Test 5 we decided to secure the bushing to the bolt by fastening an additional nut on the other side of the bushing. This was done to ensure that the bushing was an inseparable part of the bolt and hence the bolt, the nuts, and the bushing would fly out of the fixture simultaneously.

Post-mortem analysis included the examination and comparison of the sheared surfaces, the angle of the cut, and the depth of chisel penetration to the observations made in previous tests. Furthermore, measurements of weight and length of the broken bolts were completed, and the velocity of the flying portion of the bolt was determined. The time of impact of the chisel on the bolt, however, was not obtained. The scope recording that signal had been triggered prematurely, perhaps immediately prior to the bridge-wire burn out.

6. Results and Discussion

As discussed in the previous section, Summary of Tests, slight variations or departures occurred as the testing progressed. These variations or differences are described and accounted for, as we discuss and tabulate the results. The masses of the severed bolts, bushings, nuts, and washers were weighed immediately before and after each test. The initial mass and length of each bolt is reported in Table 2; post-test measurements are reported in Table 3.

The oscilloscope photos for the time-of-flight measurements are shown in Figures 7–11, along with the bridge-wire current used to detonate the explosive powder. When the current signal from the bridge-wire went to zero, there was an immediate rise in the level of detected light above that due to the He-Ne laser itself. This light was present for a time period of 1.1–1.4 ms, at which time the light level decreased and reached the 50% level. Table 4 summarizes these results. The only exceptions were in Test 1, in which the oscilloscope trace was started too late, and in Test 5 in which the bridge-wire current trigger was late, going to zero relative to the observed rise in light level, which occurred 0.75 ms prior to the drop in current. In Test 5, the 50% level must be corrected by the time the bolt

Table 2. Initial Mass and Length of Bolts Tested

Test No.	Bolt Type	Initial Bolt Mass (g)	Initial Bolt Length (cm)
1	V-Band	51.78	13.99
2	V-Band	51.82	13.98
3	DARPASAT	47.72	11.90
4	DARPASAT	47.71	11.91
5	V-Band*	55.55	15.24

*Fabricated in house from a 5/16-in. A286 stainless-steel rod

Table 3. Mass and Dimensional Properties of Severed Bolts, Bushings, Nuts, and Washers

Test No.	Mass "a" end of cut bolt Bolt, bushing, nut, washer (g)	Mass "b" end of cut bolt Bolt, bushing, nut, washer (g)	"b" bolt length (cm)	"b" end to HeNe 1 (cm) (a)*	He-Ne Separation (cm) (b)*
1	26.47, 43.36, 4.54, 1.23	29.81, 43.43, 4.53, 1.23	6.6	0.2-0.3	2.5
2	25.55, 43.36, 4, 5, 1.23	26.22, 43.43, 4.5, 1.23	7.1	0.0	1.4
3**	23.38, 43.53, 4.5, 1.23	24.21, 43.52, 0.0, 0.0	5.6	0.0	1.5
4**	23.30, 43.53, 4.5, 1.23	24.41, 43.52, 0.0, 0.0	5.6	0.0	1.7
5***	35.95, 43.56, 4.5, 1.23	19.55, 43.43, 4.5, 0.0	5.5	0.4	1.5

* Dimensions a and b are shown in the layout for the time-of-flight diagnostic, Figure 6.

** DARPASAT bolt was used, which has a bolt head on the "b" end. Neither a nut nor a washer was needed on the "b" end of the bolt.

*** Two nuts were used to lock the "b" bushing onto the bolt.

must travel to reach the first beam location. This amounted to 0.19 ms, which was negligible. Similarly, corrections for Test 1 were also negligible. No apparent trends were evident as the preload tensions of the bolts were successively lowered as the test sequence progressed.
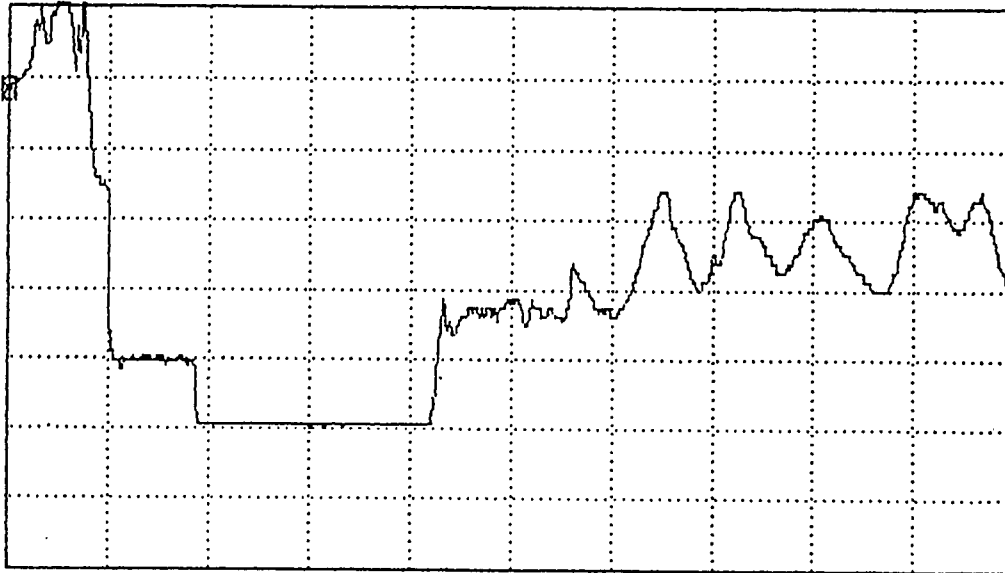
Oscilloscope Scale: 1 ms/div, 10 mv/div

Figure 7. Time-of-flight data for Test 1 at 2500 lb tension.

Oscilloscope Scale: 1 ms/div, 10 mv/div

Figure 8. Time-of-flight data and bridge-wire current trigger for Test 2 at 2250 lb tension.

20

Oscilloscope Scale: 1 ms/div, 10 mv/div

Time of flight

bridge-wire current trigger
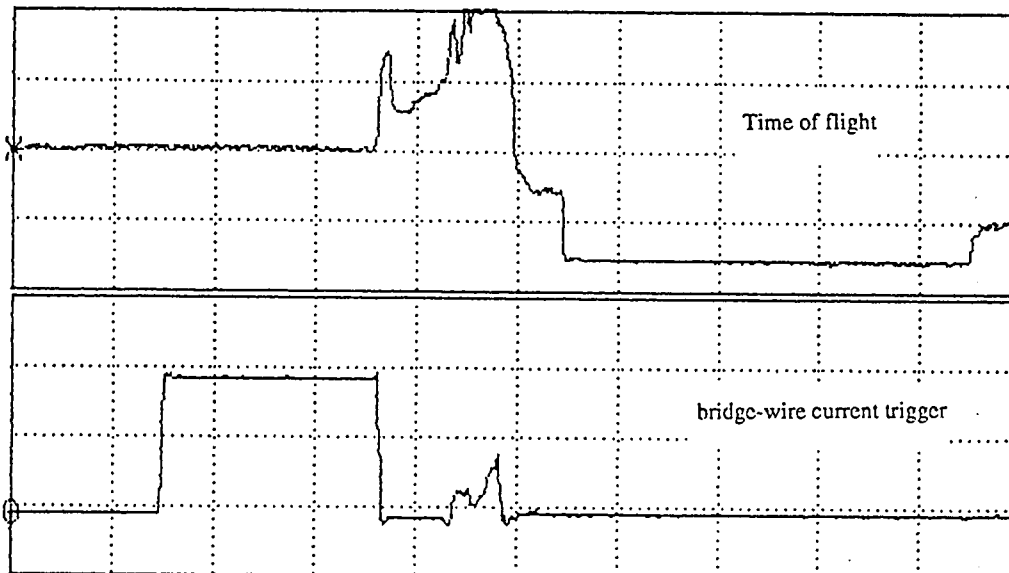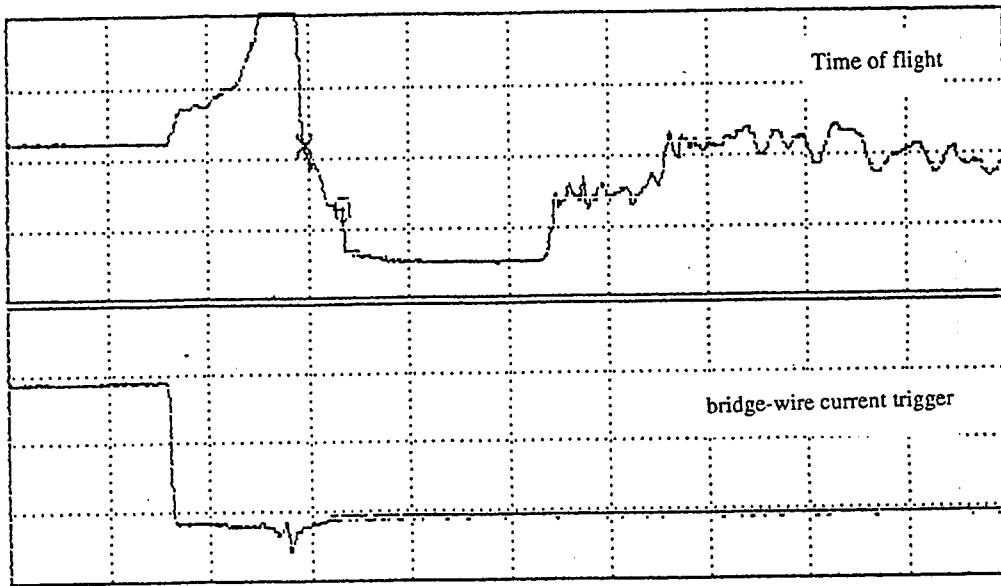
Figure 9. Time-of-flight data and bridge-wire current trigger for Test 3 at 2000 lb tension.

Oscilloscope Scale: 1 ms/div, 10 mv/div

Time of flight

bridge-wire current trigger
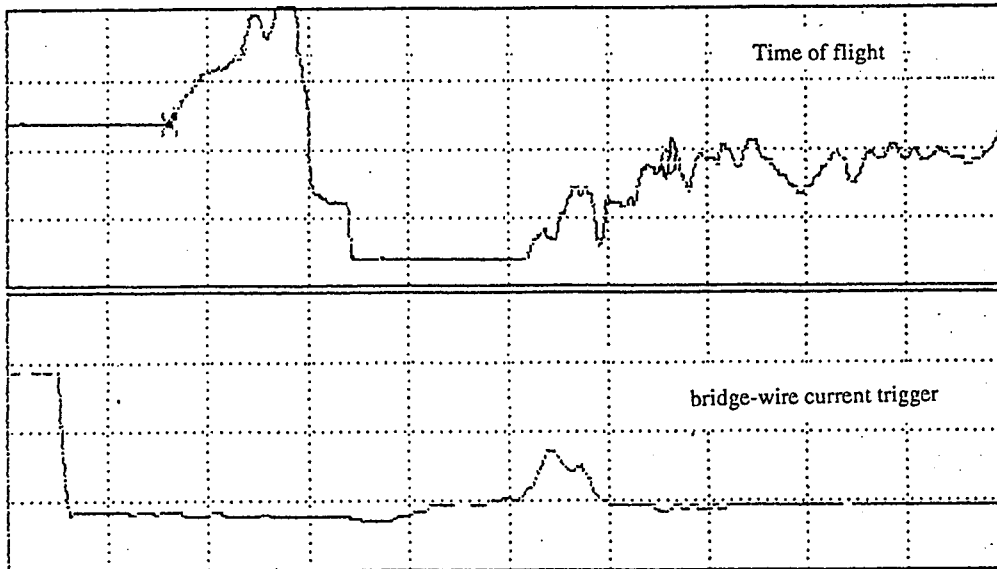
Figure 10. Time-of-flight data and bridge-wire current trigger for Test 4 at 1500 lb tension.

21
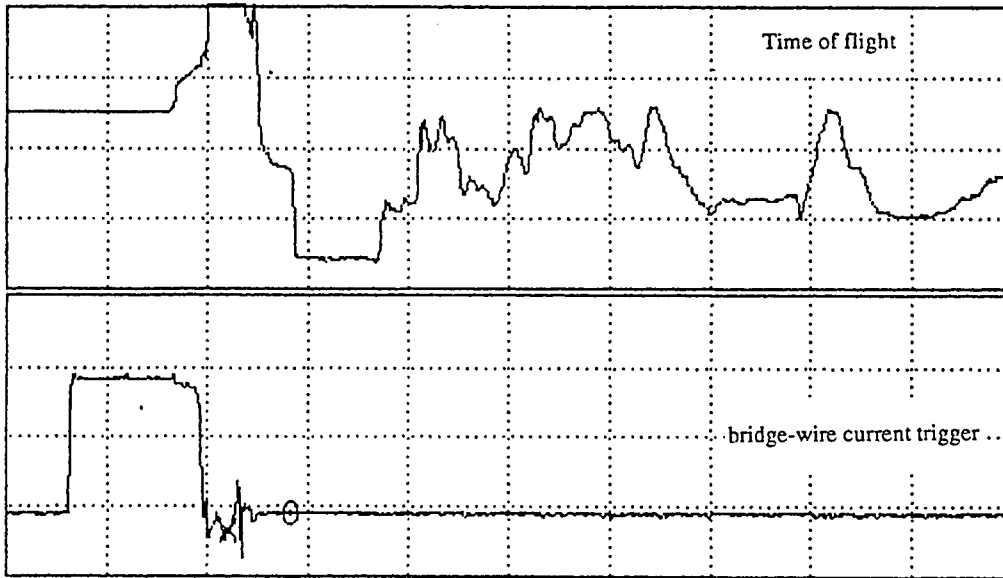
Figure 11.   Time-of-flight data and bridge-wire current trigger for Test 5 at
1000 lb tension.

Table 4.   Tension and Time Delays of Observed Light Emission and Detected
Motion of Bolt

Test No.	Loading (lb)	Time to first light (spark) (ms)*	Time to leading edge of 50% level*	Time to light max or leading offscale edge*
1	2500	---	>1.0	---
2	2250	0.0	1.36	0.90
3	2000	0.0	1.40	0.70
4	1500	<0.025	1.39	1.00
5	1000	-0.75	1.10	0.70**

* Zero reference time corresponds to falling edge of trigger current.

** Zero time corresponds to first light.

22

Some insight into the origin of the long delay times may be gleaned from the video camera records. Video camera records showed that multiple sparks might be the origin of light that increased the observed He-Ne beam intensity above the 100% level. The chisel impact on the bolt could produce light and sparks, but this zone of impact was totally enclosed within the test fixture. The observed sparks might have been produced by high-frequency vibrations of the bolt and friction in the bushings and the bushing with the cutter fixture after impact of the chisel with the bolt. The bushing was made of 17-4 precipitation-hardened stainless steel, which could promote spark formation. These sparks can be seen in Figures 12–14 for Tests 1–3. We can speculate that the cutter made contact with the bolt at the time the light intensity went off-scale. If this hypothesis is true, then the relatively long time between the peak of the light (contact of the chisel with the bolt) and the beginning motion of the bolt (breaking of He-Ne beam 1) indicates that the bolt does not fracture immediately. The time period for fracture may be as long as 0.4–0.7 ms. Only more experimentation aimed at measuring the position of the chisel as a function of time can resolve this matter. Apertures around the He-Ne beams, and placement of the He-Ne beam away from the bolt head can reduce the level of light so that the first 50% level point can be observed without this interference. Apertures were used in Tests 4 and 5. The laser beams were placed away from the bolt head in Tests 1 and 5. The use of a He-Ne filter should further reduce this light level.

The analysis of the kinetic energies (KEs) of the severed bolts involved calculating the bolt velocity and then calculating the kinetic energy. What was not known was the velocity of the bushing. Calculations were made under two assumptions to bracket the correct conclusions about the bushing velocities/energy. In the first step, at the 50% level, the KE was calculated using only the mass of the bolt, including anything firmly attached to it (but excluding the bushing). In the second assumption, all masses were accounted for, including the bushing. The identical assumptions were used for the next step segment at the 0% intensity level. These analyses were conducted for all tests; the results, however, are reported in Table 5 only for Test 1, which is representative of Tests 2–4 and for Test 5, in which the bushing was locked onto the "b" end of the bolt with the aid of nuts. The observed velocities varied from 18 to 31 m/s and is a function of the KE and mass.

Table 5. Analysis of Kinetic Energy According to Different Mass Assumptions

Test No.	Segment	Mean Velocity (m/s)	Mass Assumed (kg)	KE of Mass (J)
1	1	31.0	0.0298	14.6*
			0.07447	36.5
	2	18.0	0.0298	4.8
			0.07447	12.0*
	3	17.8	0.0298	4.7
			0.07447	11.8*
5	1	21.4	0.07195	16.8
	2	23.0	0.07195	19.0
	3	20.3	0.07195	14.8

Half Frame Images of Test 1
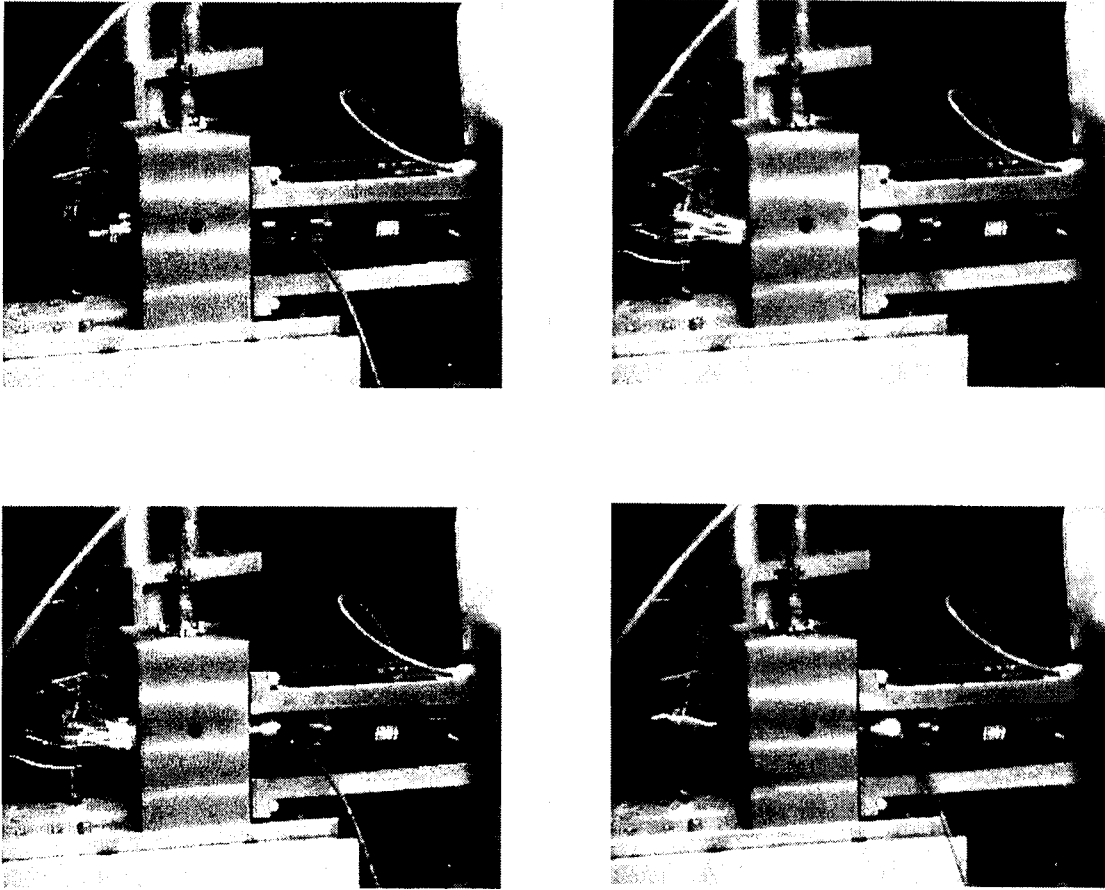
Each image is integrated for 1/60 s

Figure 12. Video-frame photo of Test 1 from a Sony black and white video camera(XC-57). The half frame sequence in upper left is 1, lower left is 2, upper right is 3, and lower right is 4. The first half frame is taken before impact. Each half frame is 1/60 s.

Half Frame Images of Test 2

Each image is integrated for 1/60 s

Figure 13. Video-frame photo of Test 2 from a Sony black and white video camera (XC-57). The half frame sequence in upper left is 1, lower left is 2, upper right is 3, and lower right is 4. The first half frame is taken before impact. Each half frame is 1/60 s.
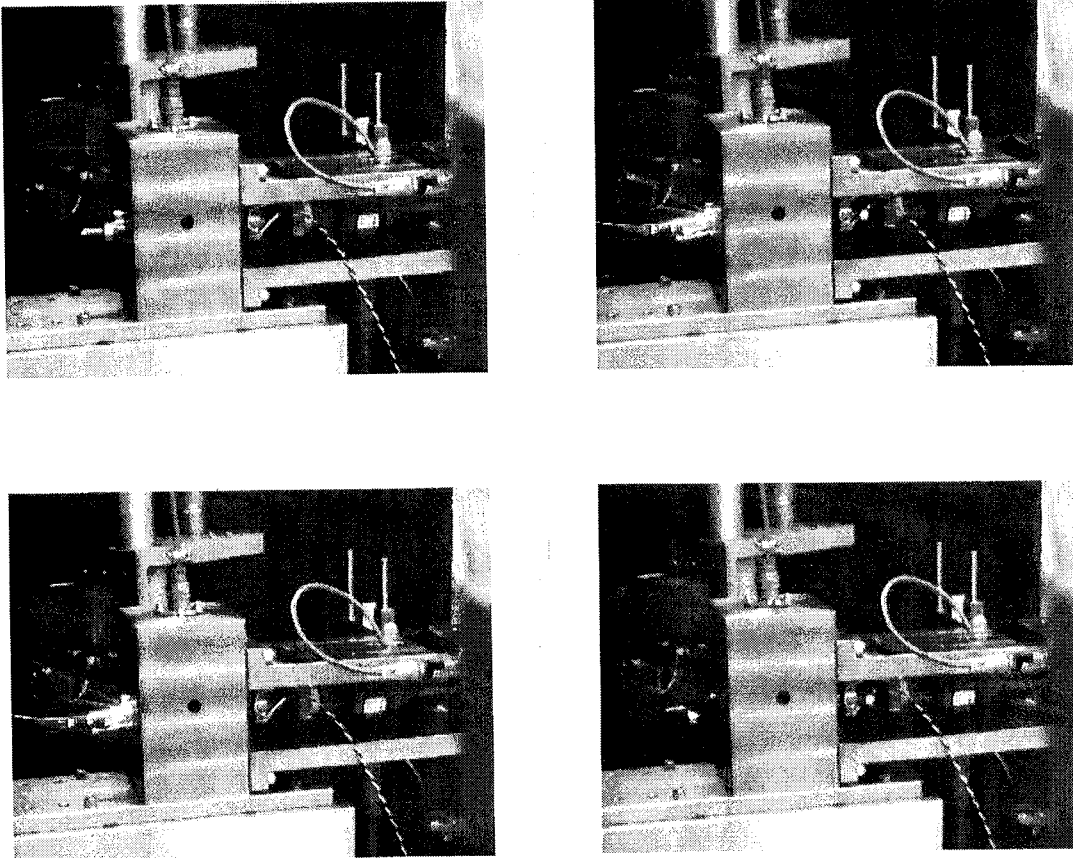
25

Half Frame Images of Test 3

Each image is integrated for 1/60 s

Figure 14. Video-frame photo of Test 3 from a Sony black and white video
            camera(XC-57). The half frame sequence in upper left is 1, lower
            left is 2, upper right is 3, and lower right is 4. The first half frame
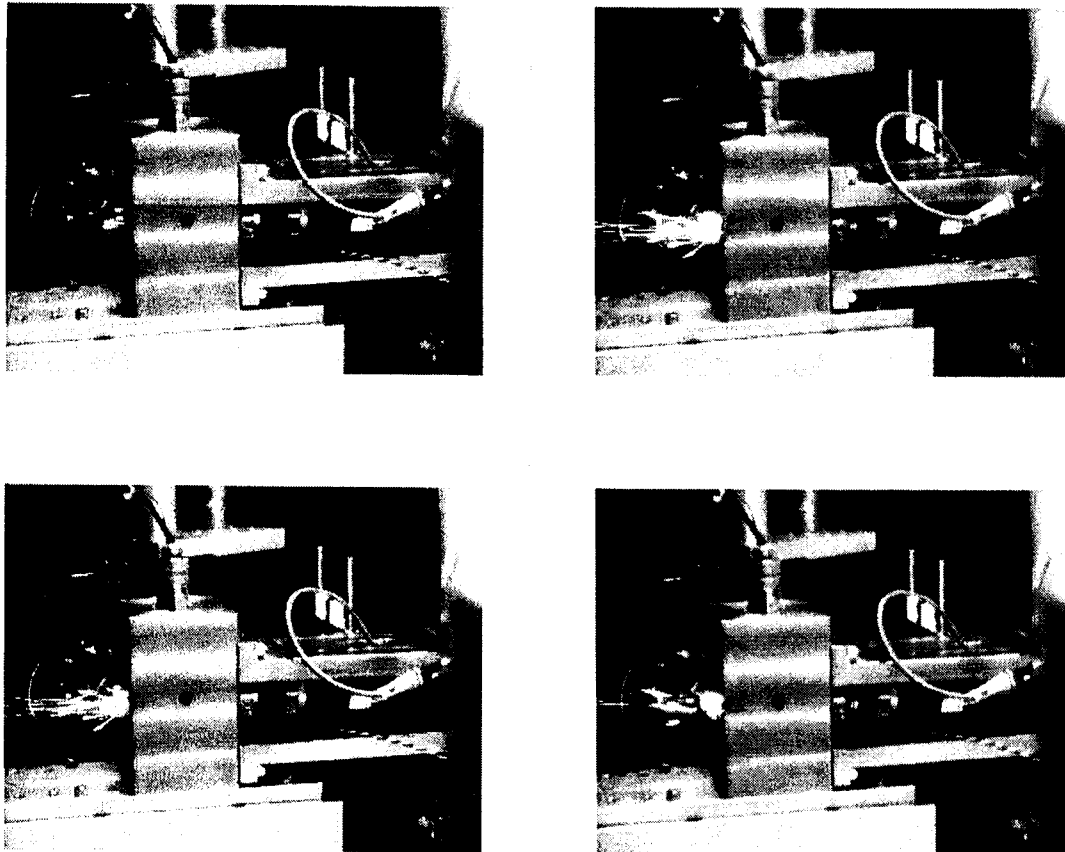   is taken before impact. Each half frame is 1/60 s.

It is clear that in segment 1, the bushing is carrying a negligible amount of KE, and that in the second
and subsequent segments, the bushing is accelerated to nearly the same velocity and energy as the
bolt. The estimated accuracy in the energy estimation is ± 20%. Thus, energy conservation is
verified.

We assume this scenario from Table 5 in reporting the velocity and energy of the bolt fragments. The
mass, velocities, and time duration of each step segment for the bolt fragments and the kinetic ener-
gies calculated using Eq. (3) are given in Table 6.

26

Table 6. Mass, Velocity, and Kinetic Energy for Each Bolt Fragment

Test No.	Segment	Segment Time (ms)	Velocity (m/s)	Mass a, b (g)	KE$_b$ (J)	KE$_{total}$ (J)	Chisel KE Fraction (%)**
1	1	0.80	31.0	30.1, 29.8	14.6	29.1	15
	2	2.5	18.0	30.1, 74.47	12.0	41.7	22
	3	1.4	17.8	30.1, 74.47	11.8	41.0	22
2	1	0.49	28.6	30.0, 30.7	12.5	25.3	13
	2	4.07	14.0	30.0, 75.38	7.37	25.9	14
	3	---	---	30.0, 75.38	---	---	---
3	1	0.36	41.7	28.8, 24.2	21.0	38.6	20
	2	2.07	19.8	28.8, 67.81	13.3	44.6	23
	3	1.12	13.4	28.8, 67.81	6.08	20.4	11
4*	1	0.41	41.5	27.8, 24.41	21.0	39.4	21
	2	1.80	21.7	27.8, 67.94	16.0	54.9	29
	3	1.09	15.6	27.8, 67.94	8.3	28.7	15
5*	1	0.70	21.4	35.95, 71.95	16.8	49.5	26
	2	1.74	23.0	35.95, 71.95	19.0	57.0	30
	3	0.74	20.3	35.95, 71.95	14.8	44.4	23

* Apertures were added to reduce light pick-up by the photodiode.

** Assumes initial chisel kinetic energy before impact is 190 J.

Observed velocities may vary due to the effect of the additional emitted light, which raises the signal level early at the leading edge of the first step, which produces a shorter time for the first step (50% level). In turn, a higher velocity and kinetic energy would be inferred. But in every test, the energy is within agreement or somewhat lower for the first segment relative to the second segment. We can conclude that emitted-light effects can be ignored. Energy conservation for segment three is fairly good.

Overall, the data of Table 6 show that energy is conserved, using the assumptions of bolt only for Step 1 and bolt plus bushing for Step 2 and Step 3 for the kinetic energy analysis. Of the original 190 J of the chisel, the fraction of transferred energy varies by a factor of nearly 3, from 11 to 30%, from test to test. This observed variation may be the result of a unusually low values in some of the tests and a trend in the data as the preload tension on the bolt is lowered. A plot of the kinetic energy as a function of the bolt tension is shown in Figure 15. The plot shows a trend towards higher kinetic energy as the tension is lowered over the tension range investigated. A least-squares fit to a straight line yields a slope of -0.0113 ± 0.0047 J/lb, and a intercept of 59 ± 9 J. Whether this trend is borne out at lower tension values is unknown, and future experiments may address this energy distribution as a function of the testing conditions including higher and lower values for preload tension. Test 5, in which the bushing was attached to the bolt, gave very consistent values for the velocity, indicating that the uncertainty due to the unknown bushing velocity was absent. It also has the smallest relative variance in KE for all test shots.
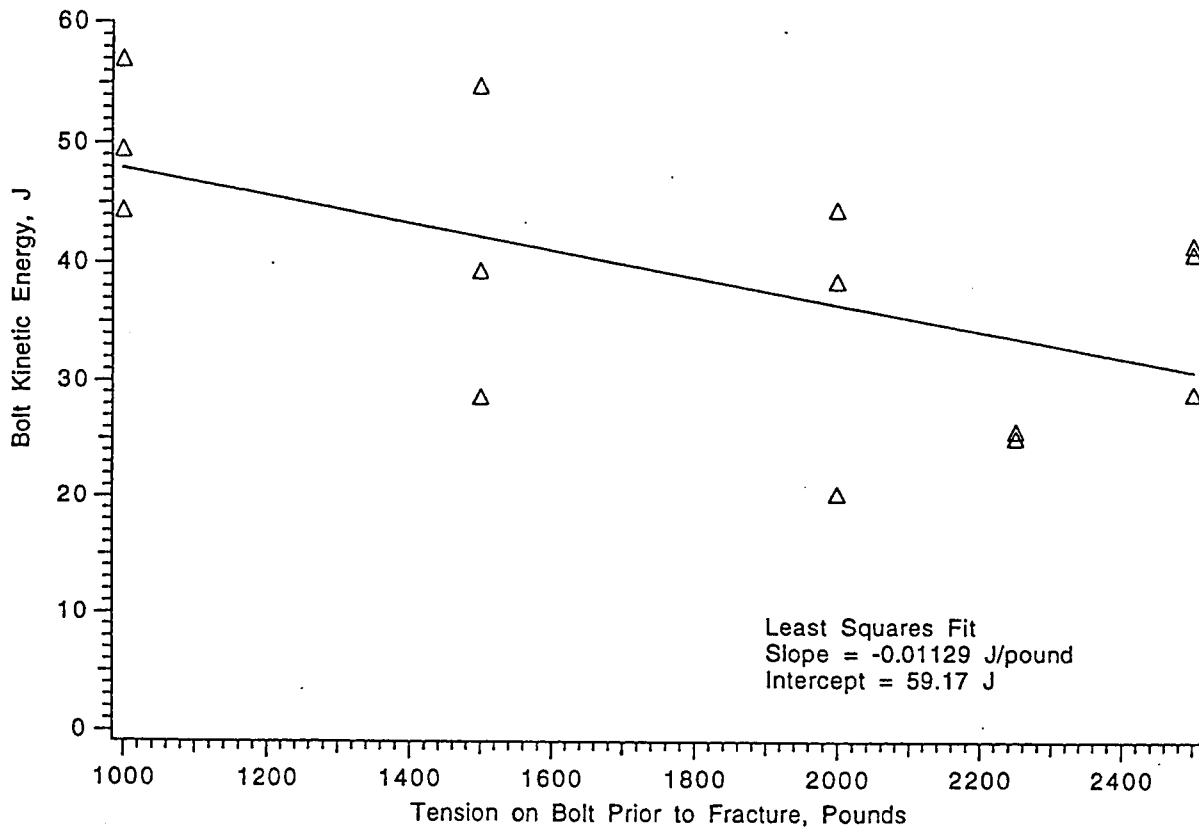
Figure 15. Dependence of the kinetic energy of severed bolts on pre-load tension. The data show that over the range of preload tension investigated (1000 to 2500 lb) the kinetic energy transferred to the severed bolt is slightly increasing as the tension is lowered. The cause of this effect is not known.

6.1   Video Camera Diagnostic Results

Video-taped images were time-base corrected, digitized, and printed. The photos are taken off each half frame or field with an exposure time of 1/60 s for each frame. Images from Tests 1–3 are displayed in Figures 12–14. In Tests 4 and 5, a white sheet of paper was used to form apertures for He-Ne beams 1 and 2. The aperture, while effective in blocking light from the sparks, obscured the observation of the sparks due to overexposure. The velocity of the bolt is too high to be observed and for useful bolt images to be analyzed. The entire cutting phenomena is over within two half frames. What is most evident in all tests performed is a shower of sparks that seem to originate about the bolt and bushing, which moves in the bolt and bushing flyout direction(toward the left as viewed). A black sheet of paper is recommended as the aperture to prevent obscuration of the sparks as observed in Tests 4 and 5.

6.2   Examination of Cut Surfaces

Post-mortem examination of all severed bolts led to the following observations:

1. For all tests, the chisel penetrated slightly more than half-way through the bolt's diameter; the bolts were severed by fracture.

2. The depth of chisel penetration could easily be recognized since cut surfaces were shiny, and evidence of plastic deformation (so-called adiabatic shear) was present.

3. The fractured surfaces were rough and oriented in classical 45° planes relative to the direction of the cut.

4. There were no appreciable differences between the cut surfaces from test to test. The orientation and roughness of the cut or fractured surfaces, as well as the depth of blade penetration, were similar in all five cases. This suggests that the V-band bolts, the DARPASAT bolts, and the in-house-made bolt were metallurgically the same and dimensionally equal. Moreover, the tension in the bolt didn't appear to affect the depth of blade penetration. The similarity between the cut surfaces also suggest that the cutters were all functionally the same and in one family.

5. If the tension in the bolt doesn't affect the penetration depth, then one should expect that similar bolts could be severed by these cutters under no tension. In other words, reasons other than bolt tension must exist to explain why some of the bolts weren't severed in the contractor's tests.

Figure 16 is a photograph of a typical severed bolt, showing both the cut and the fractured side of the bolt. Both fractured pieces are shown in this figure. The indentation made by the anvil as the chisel impacts the bolt is clearly seen on the bolt.
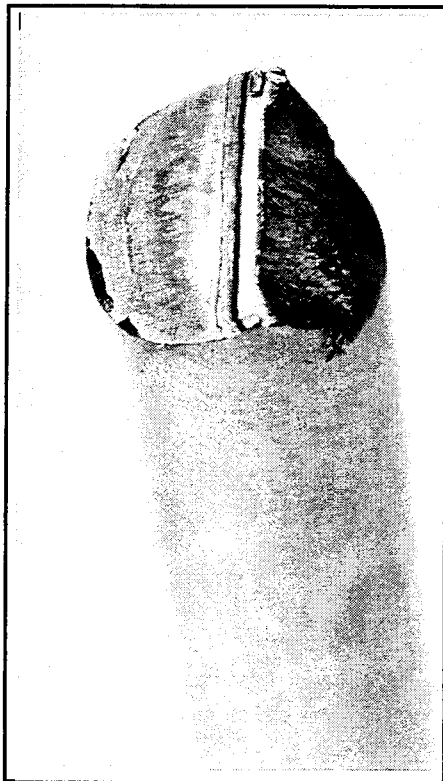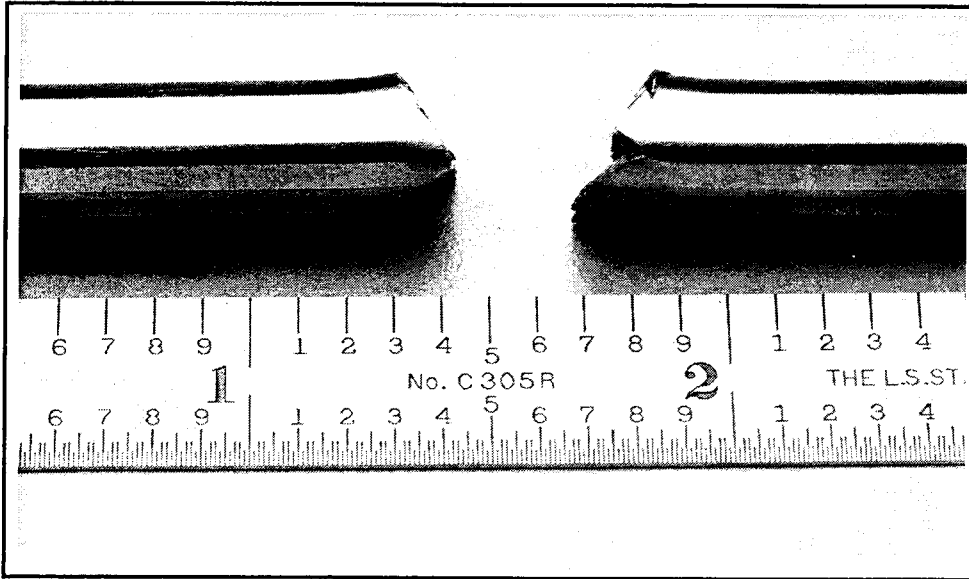
Figure 16.   Photograph of a typical severed bolt showing the cut and the
fractured side of the both fractured pieces.

30

7. Conclusions and Recommendations

First and foremost, the bolts were successfully severed in all five tests. It was shown that the cutters are capable of successfully severing this class of bolts even when subjected to a preload as low as 1000 lb. This demonstrates a substantial margin relative to the nominally set preload value of 3200 lb. Post-mortem examination of the cut surfaces showed no correlation between the bolt preload and the chisel penetration depth.

Velocity measurements on the "b" end of severed bolts indicate that 30 to 50 J of energy was present in the KE of the bolt fragments. Some uncertainty was present in the data arising from the bushing KE uncertainty. However, the data indicate that energy conservation is obeyed if assumptions about the bushing KE are properly made. Up to 30% of the chisel KE appears to be transferred to bolt fragment KE. There is a slight trend in the data that suggests that the bolt KE increases as the pre-load tension on the bolt is decreased over the tension range of 2500 to 1000 pounds. Measured "b" end bolt velocities varied from 21 to 42 m/s in the step segment 1 down to 14 to 20 m/s in the step segment 3.

If the test conditions allow, it is highly recommended that an additional diagnostic be used to monitor the chisel position as a function of time in addition to the bolt time of flight. Using data from this diagnostic, the chisel velocity before and after bolt fracture can be measured to formulate an energy distribution budget in conjunction with the bolt time-of-flight data. This will allow inferrence of the energy of the plastic deformation and the distribution of the initial chisel kinetic energy as a function of the initial bolt tension. The exact time of chisel impact on the bolt and the time of bolt fracture can be measured. This will explain the long observed times between the peak of the emitted light and motion of the "b" bolt end. A He-Ne filter and apertures could reduce the interference of emitted light.

One way to implement this new diagnostic is to put a long slot in the bolt cutter assembly to allow a beam with an elongated cross section to traverse the space above the bolt. Calibration would allow conversion of amplitude information into position of the chisel. Another implementation would be to use a series of white stripes on the side of the chisel to scatter light from a laser, which provides a position tick mark recorded as a function of time. A fiber-optic cable could be used to transmit and receive the scattered laser light and could be located close to the chisel to exclude light from sparks thrown at the time of chisel impact.

The time-of-flight experiment should be undertaken using a bushing that is rigidly attached to the bolt to eliminate uncertainty in the bushing KE contribution to the total KE in the bolt fragments. Variations in frictional effects that affect the KE transfer are also avoided.

TECHNOLOGY OPERATIONS

The Aerospace Corporation functions as an "architect-engineer" for national security programs, specializing in advanced military space systems. The Corporation's Technology Operations supports the effective and timely development and operation of national security systems through scientific research and the application of advanced technology. Vital to the success of the Corporation is the technical staff's wide-ranging expertise and its ability to stay abreast of new technological developments and program support issues associated with rapidly evolving space systems. Contributing capabilities are provided by these individual Technology Centers:

Electronics Technology Center: Microelectronics, solid-state device physics, VLSI reliability, compound semiconductors, radiation hardening, data storage technologies, infrared detector devices and testing; electro-optics, quantum electronics, solid-state lasers, optical propagation and communications; cw and pulsed chemical laser development, optical resonators, beam control, atmospheric propagation, and laser effects and countermeasures; atomic frequency standards, applied laser spectroscopy, laser chemistry, laser optoelectronics, phase conjugation and coherent imaging, solar cell physics, battery electrochemistry, battery testing and evaluation.

Mechanics and Materials Technology Center: Evaluation and characterization of new materials: metals, alloys, ceramics, polymers and their composites, and new forms of carbon; development and analysis of thin films and deposition techniques; nondestructive evaluation, component failure analysis and reliability; fracture mechanics and stress corrosion; development and evaluation of hardened components; analysis and evaluation of materials at cryogenic and elevated temperatures; launch vehicle and reentry fluid mechanics, heat transfer and flight dynamics; chemical and electric propulsion; spacecraft structural mechanics, spacecraft survivability and vulnerability assessment; contamination, thermal and structural control; high temperature thermomechanics, gas kinetics and radiation; lubrication and surface phenomena.

Space and Environment Technology Center: Magnetospheric, auroral and cosmic ray physics, wave-particle interactions, magnetospheric plasma waves; atmospheric and ionospheric physics, density and composition of the upper atmosphere, remote sensing using atmospheric radiation; solar physics, infrared astronomy, infrared signature analysis; effects of solar activity, magnetic storms and nuclear explosions on the earth's atmosphere, ionosphere and magnetosphere; effects of electromagnetic and particulate radiations on space systems; space instrumentation; propellant chemistry, chemical dynamics, environmental chemistry, trace detection; atmospheric chemical reactions, atmospheric optics, light scattering, state-specific chemical reactions and radiative signatures of missile plumes, and sensor out-of-field-of-view rejection.